

# Algorithms for Cameras View-Frame Placement Problems in the Presence of an Adversary and Distributional Ambiguity\*

Seonghun Park<sup>1</sup> and Manish Bansal<sup>†1</sup>

<sup>1</sup>*Grado Department of Industrial and Systems Engineering,  
Virginia Tech, Blacksburg, VA, 24061, USA*

April, 2023

## Abstract

In this paper, we introduce cameras view-frame placement problem (denoted by CFP) in the presence an adversary whose objective is to minimize the maximum coverage by  $p$  cameras in response to input provided by  $n$  autonomous agents in a remote location. We allow uncertainty in the success of attacks, incomplete information of the probability distribution associated with the uncertain data, and varying levels of risk-appetite of the adversary. We present an exact cutting planes based algorithm to solve this problem along with conditions under which it is finitely convergent. Since this approach solves deterministic CFP in each iteration, we also present improved exact method for CFP with  $p = 1$ , approximation algorithm and heuristics for Multi-CFP with  $p \geq 2$ , and Multi-CFP with fixed tilt of the cameras. To evaluate the effectiveness and performance of the proposed approaches, we conduct computational experiments using randomly generated instances and simulation experiments where these approaches are utilized to find a hidden object in a remote location.

*Note to Practitioners*– This paper is motivated from application of cameras view-frame placement problem for military surveillance and reconnaissance in the presence of an adversary. We formulate this problem as a game played between an attacker and the camera-system user that captures uncertainty in the success of attacks and risk-appetite of the players. Its optimal solution, obtained using the proposed solution approaches, provides insight to both decision-makers/players. Especially, the camera-system user can identify the set of agents that are susceptible to attacks by a reasonable (risk-averse) attacker, and hence, can plan to have backup agents as well. Likewise, the proposed algebraic modeling framework and solution approaches are also applicable for planning interdiction actions to minimize the information acquisition by an evader/enemy.

*Keywords:* adversarial camera view-frame placement, distributionally robust optimization, pan-tilt-zoom cameras, exact and approximate algorithm, cutting planes

---

\*Distribution A. Approved for public release; distribution unlimited. OPSEC # 7408

<sup>†</sup>Corresponding author (bansal@vt.edu)

# 1 Introduction

Telerobotic cameras (standalone or installed on autonomous ground/aerial vehicles and satellites) enable multiple users and researchers in healthcare [10], distance learning, natural environment observation [18], surveillance [15, 13], and space exploration [7], to interact with a remote physical environment using shared resources. They provide information (videos and images) to decision makers for conducting operations such as intelligence, surveillance and reconnaissance, in environment where it is tedious for humans to collect information. Oftentimes, there are multiple ( $n$ ) agents in the remote region to inform a decision maker about potential regions of threat along with the intensity of the threat. However, given a limited number of cameras ( $p \ll n$ ) with adjustable pan, tilt, and zoom, the decision maker can focus the view-frame of the cameras on only a subset of these regions such that subregions with maximum threat (or reward) are covered, in a given time window. Moreover, in adversarial environment, the agents are likely to be attacked or incapacitated by an adversary whose aim is to minimize the maximum information acquisition by the decision maker. This leads to a game played between two players (or decision-makers): an attacker and a defender. Because of limited resources, the attacker attacks a subset of the agents with the objective of minimizing the defender’s maximization objective. The defender has a “wait and see” strategy, i.e., they use input from the agents after observing success or failure of the attacks, and then decide location and dimensions of cameras rectangular view-frame by adjusting pan, tilt, and zoom of the cameras such that maximum reward is covered.

In this paper, we consider uncertainty in the success of the attacks on the agents and represent it using a random variable defined over a sample space (a set of events or realizations of the random variable). In case probability distribution associated with this variable is known, the adversary’s objective is to minimize the expected maximum covered reward of the defender. However, in many applications such as military operations, availability of probability of occurrence of the events is limited. To tackle this aspect of uncertainty, we construct a set of distributions (referred to as ambiguity set) using the limited knowledge such as bounds on mean, variance, and/or higher order moments, and then define the adversary’s objective as minimizing the expected maximum covered reward function for the worst-case probability distribution within the ambiguity set. By solving this problem, the defender gets information about vulnerable agents whose destruction can significantly impact their objective. Observe that by adjusting the ambiguity set, this framework also allows adjustments based on varying levels of risk-appetite of the adversary.

Mathematically, the adversarial camera-view frame placement problem is defined as follows. Let  $N = \{1, \dots, n\}$  be a set of  $n$  agents, and  $\sigma = (\sigma_1, \dots, \sigma_n) \in \{0, 1\}^n$  denotes adversary’s decision variables:  $\sigma_i = 1$  if agent  $i$  is attacked, and 0 otherwise. Given the maximum number of agents the adversary can attack, i.e.,  $b$ , the adversary’s objective is

$$\min_{\sigma \in \{0,1\}^n} \left\{ \Phi(\sigma) := \max_{P \in \mathcal{P}} \mathbb{E}_P[Q(\sigma, \xi)] \mid \sum_{i=1}^n \sigma_i \leq b \right\} \quad (1)$$

where  $\mathcal{P}$  denotes the ambiguity set,  $\mathbb{E}_P[\cdot]$  and  $\xi$  are expectation operator and random variable with distribution  $P$ , respectively. Function  $Q(\sigma, \xi)$  returns defender’s optimal objective function value for given  $\sigma$  and each realization of  $\xi$ ; refer to Section 1.3 for more details

about  $Q(\cdot)$ . Notice that the inner maximization is to find decisions for worst-case probability distribution within  $\mathcal{P}$ , thereby providing distributionally risk-averse (or robust) solution. For  $|\mathcal{P}| = 1$ , formulation (1) reduces to risk-neutral problem, and when  $\mathcal{P}$  is defined by all probability distributions supported on the sample space of  $\xi$ , it reduces to robust optimization model where adversary makes most-conservative risk-averse decisions for the worst-case realization of the random variable  $\xi$ .

## 1.1 Literature Review

Only special cases of problem (1) in the absence of any adversary (i.e.,  $b = 0$ ) have been studied in the literature [2, 15, 14, 20]. Specifically, Song et al. [15] introduced camera view-frame placement problem (denoted by CFP) with single camera in the context of satellite imaging where the camera/satellite receives a rectangular region as request from each of the  $n$  users along with reward rate (per-unit area) for each request. They presented exact algorithms for placing rectangular view-frame of the camera and selecting its resolution level such that maximum reward is covered. Note that the resolution level impacts dimensions of the view-frame and reward rate of covered requests. Xu et al. [19] provided an exact algorithm for CFP with two cameras having non-overlapping view-frames. Bansal and Kianfar [2] proved that CFP with  $p$  cameras is NP-hard if  $p$  is a part of the input, and presented an exact algorithm for this problem under the assumption that all cameras have same and fixed resolution level. Approximation algorithms have also been developed for CFP with polygon shape of the requests [14, 20]. In this paper, we present theoretical results that improve the efficiency of exact algorithms by [15] for CFP with single camera along with heuristics, approximation algorithms for CFP with multiple cameras having continuous resolution levels.

*Relation of CFP with Other Computational Geometry Problems.* For the sake of completeness, we also review computational geometry problems related to CFP, in particular planar maximum coverage location problems (PMCLP) with Manhattan distances. This problem is analogous to CFP with points as requests and squares having fixed dimensions as view-frames to represent demand and service zone of a facility with fixed service range, respectively. The goal of PMCLP is to find location of these facilities anywhere on a two-dimensional plane such that maximum demand is covered by them [5, 11, 16]. Murray and Tong [12] presented a binary formulation for an extension of PMCLP with line segments and polygon as requests under an assumption that view-frames can either completely cover the requests or not covered at all. Bansal and Kianfar [2] relaxed this assumption by allowing partial overlap between the (rectangular) requests and view-frames, thereby leading to CFP with multiple cameras. Both of these studies assume that the view-frames have fixed and same dimensions.

In another direction, optimization problems involving two non-cooperating players who play a zero-sum Stackelberg game are well-known in the context of network interdiction [6, 8]. In these games, an interdictor (also referred to as leader or adversary) attacks arcs and/or nodes of a network that is used by an evader (also referred to as follower or defender) to transport illegal drugs or nuclear material. The goal of the evader is to either maximize the flow [17] or minimize the shortest path [8] from source node to destination node, and the interdictor's aim is to minimize or maximize, respectively, the evader's objective. Since the

flow maximization and shortest path problems can be formulated as linear programs, the dual of these linear program are being utilized to get either lower-bound approximation of  $Q(\sigma, \xi)$  or an overall monolithic minimization problem. In contrast, no explicit (or closed form) definition of functions  $Q(\sigma, \xi)$  and  $\Phi(\sigma)$  in Problem (1) is known. Moreover, most of these network interdiction literature assumes that either all data parameters or complete description of the probability distribution are known, except in [9] where formulation akin to (1) is considered to relax the foregoing assumption in the aforementioned shortest path network interdiction problem.

## 1.2 Contributions and Organization of this Paper

As per our knowledge, no solution approach is known in the literature for solving formulation (1), primarily because no explicit (or closed form) definition of functions  $Q(\sigma, \xi)$  and  $\Phi(\sigma)$  is known. Therefore, we first introduce a class of valid inequalities to derive lower-bound approximation of function  $\Phi(\sigma)$ . We then embed these cuts within a branch-and-cut based decomposition algorithm to exactly solve this problem, and provide conditions under which this algorithm is finitely convergent (Section 2). Since this approach solves deterministic CFP (in the absence of uncertainty and adversary) in each iteration, we also introduce computationally efficient solution approaches for solving CFP with single and multiple cameras.

Specifically, we consider algorithms by [15] for single camera with reduced solution search space, thereby making them four times faster (Section 3). In Section 4, we present two heuristics (greedy and clustering-based methods) for CFP with multiple cameras and a heuristic for CFP with two cameras. Also, we prove that the approximation ratio of the greedy method is  $1 - 1/e$  where  $e$  is natural logarithm constant (or Euler’s number). Lastly, for CFP with multiple cameras having fixed tilt, a finite set of values for pan and adjustable zoom, we provide an heuristic algorithm to solve it (Section 5). Note that this special case has applications in street/border/river surveillance.

To evaluate the effectiveness and performance of the proposed approaches, we conduct computational experiments using randomly generated instances and simulation experiments where these approaches are utilized to find a hidden object in a remote location (Section 6). In Section 8, we provide concluding remarks and potential future research directions.

## 1.3 Notations and Definitions

In this section, we formally define defender’s problem, i.e.,  $Q(\sigma, \xi)$ , along with other notations and definitions needed for the algorithms presented in the ensuing sections.

**Definition 1.1.** *Let  $d_i$  denotes a rectangular region requested by agent  $i \in N := \{1, \dots, n\}$ , that is defined by coordinates of its lower left corner  $(x_i, y_i)$ , width  $w_i$ , height  $h_i$ , reward rate  $r_i$  (per-unit area), and desired resolution  $z_i$ . Define  $\mathcal{D} = \{d_i, i \in N\}$  as set of all requests.*

It is important to note that the proposed solution approach for solving (1) is applicable for any spatial region (polygon, circle, etc.) as request by an agent. For simplicity of exposition, we present results for only rectangular requests.

**Definition 1.2.** Rectangular view-frame of camera  $j \in \{1, \dots, p\}$  is denoted by  $s_j = [(x_{s_j}, y_{s_j}), w_{s_j}, h_{s_j}, z_{s_j}]$  where coordinates of its lower left corner  $(x_{s_j}, y_{s_j})$ , width  $w_{s_j}$ , height  $h_{s_j}$ , and resolution  $z_{s_j}$  are unknown. Width and height of  $s_j$  depend on its resolution, i.e., the size of the view-frame increases as  $z_{s_j}$  increases, but the quality of the information (image or video) decreases. Define  $\mathcal{S} := \{s_1, \dots, s_p\}$ .

**Definition 1.3** ([15]). Let  $\alpha_i = \frac{z_i}{z_s}$  for request  $d_i$  and view-frame  $s$ . Define discount function  $g(\alpha_i)$  that satisfies the conditions:

- $g(\alpha_i) = 1$ , when  $\alpha_i \geq 1$ ;
- $0 \leq g(\alpha_i) \leq 1$ , when  $\alpha_i \leq 1$ ;
- $g(\alpha_i)$  is an increasing function.

Normally,  $g(\alpha_i) = \min\{(\alpha_i)^b, 1\}$  where  $b$  is some constant. Assume  $b = 1$ , the reward from request  $d_i$  covered by camera frame  $s \in \mathcal{S}$  with resolution level  $z_s$  is equal to  $r_i A(d_i \cap s) g(\alpha_i) = r_i A(d_i \cap s) \min\{\alpha_i, 1\}$  where  $A(\cdot)$  returns the area of its argument.

**Definition 1.4.** Function  $\mathcal{R}(d_i \cap (\cup_{j=1}^p s_j))$  returns reward from request  $d_i$  covered by the union of  $p$  camera-view frames  $s_j \in \mathcal{S}$  with resolution level  $z_{s_j}$  for  $j \in \{1, \dots, p\}$ .

Let  $\Omega := \{\omega_1, \dots, \omega_{|\Omega|}\}$  be a finite set of possible realizations of the random variable  $\xi \in \{0, 1\}^n$ . Each realization  $\xi^\omega \in \{0, 1\}^n$  of the random variable occurs with probability  $\bar{p}_\omega$  where  $\xi_i^\omega = 1$  (or  $\xi_i^\omega = 0$ ) implies the success (or failure) of attack on agent  $i \in N$ . For  $\omega \in \Omega$ , let  $\mu_i^\omega \in \mathbb{R}_+$  denotes the total reward from request  $d_i$  captured by  $p$  view-frames with given position and resolution in scenario  $\omega \in \Omega$ . We refer to  $\mu^\omega \in \mathbb{R}_+^n$  as reward-coverage vector. Since the defender cannot get any reward from request  $d_i$  in case the attack on agent  $i$  is successful,  $\mu_i^\omega \leq r_i w_i h_i (1 - \sigma_i \xi_i^\omega)$  for all  $i \in N$  and  $\omega \in \Omega$ . Note that optimal covered-reward  $\mu_i^{\omega*} = \mathcal{R}(d_i \cap (\cup_{j=1}^p s_{j,\omega}^*))$  where  $\{s_{j,\omega}^*\}_{j=1}^p$  denotes an optimal solution of the defender in scenario  $\omega \in \Omega$ , and

$$Q(\sigma, \omega) = \sum_{i \in I_\omega} \mu_i^{\omega*} \quad \text{where } I_\omega := \{i \in N : \sigma_i \xi_i^\omega = 0\}.$$

We assume that the probability distribution  $\{\bar{p}_\omega\}_{\omega \in \Omega}$  of the random variable  $\xi$  belongs to an ambiguity set  $\mathcal{P}$ . In the literature, this set has been defined in different way; refer to [3, 1, 9] and references therein. We present algorithm that will be applicable to any definition of the ambiguity set. Only for our computational experiments, we restrict the first  $m$  moments of the random variable within predetermined bounds to get a so-called moment matching set:

$$\mathcal{P} = \left\{ \left\{ p_\omega \right\}_{\omega \in \Omega} : l_q \leq \sum_{\omega \in \Omega} p_\omega v_q(\omega) \leq u_q \text{ for } q = 1, \dots, m; \right. \\ \left. \sum_{\omega \in \Omega} p_\omega = 1; p_\omega \geq 0 \forall \omega \in \Omega \right\},$$

where  $l_q$  and  $u_q$  denote the predetermined lower bound and upper bound vector on  $q$ th moment vector of random variable for restricting the moments, and  $v_q$  is a measurable function defined on  $\Omega$  and its sigma-algebra  $\mathcal{F}$ .

## 2 Adversarial Cameras View-Frame Placement Problem with Distributional Ambiguity

We first present a family of valid inequalities in the following theorem that provides lower bound approximations for the function  $\Phi(\sigma)$ . Then, we incorporate these inequalities in a decomposition framework to solve the original problem (1).

**Theorem 2.1.** *Given an adversary's solution  $\tilde{\sigma} \in \mathcal{X} := \{\sigma \in \{0, 1\}^n : \sum_{i \in N} \sigma_i \leq b\}$  and the associated defender's optimal reward-coverage vector  $\tilde{\mu}^\omega$  for  $\omega \in \Omega$ , the inequality:*

$$\Phi(\sigma) \geq \Phi(\tilde{\sigma}) - \sum_{i \in N} \sum_{\omega \in \Omega} \tilde{p}_\omega \tilde{\mu}_i^\omega \xi_i^\omega \sigma_i \quad (2)$$

where  $\{\tilde{p}\}_{\omega \in \Omega} = \arg \max_{\{p_\omega\}_{\omega \in \Omega}} \sum_{\omega \in \Omega} p_\omega Q(\tilde{\sigma}, \omega)$ , is valid for  $\sigma \in \mathcal{X}$ .

*Proof.* Given  $\tilde{\sigma} \in \mathcal{X}$  and scenario  $\omega \in \Omega$ , let  $\tilde{I}_\omega := \{i \in N : \tilde{\sigma}_i \xi_i^\omega = 0\}$  be the set of agents/requests that are not impacted by adversary's solution  $\tilde{\sigma}$ , and an optimal defender's solution and associated reward-coverage vector be denoted by  $\tilde{\mathcal{S}}^\omega = (\tilde{s}_1^\omega, \dots, \tilde{s}_p^\omega)$  and  $\tilde{\mu}^\omega$ , respectively. For any  $\sigma \in \mathcal{X}$ , define reward-coverage vector  $\bar{\mu}^\omega$  that returns reward from requests in  $I_\omega = \{i \in N : \sigma_i \xi_i^\omega = 0\}$  covered by  $\tilde{\mathcal{S}}^\omega$ , i.e.,

$$\bar{\mu}_i^\omega = \begin{cases} \tilde{\mu}_i^\omega, & \text{if } i \in I_\omega \cap \tilde{I}_\omega \\ \mathcal{R}(d_i \cap (\cup_{j=1}^p \tilde{s}_j^\omega)), & \text{if } i \in I_\omega \setminus \tilde{I}_\omega \\ 0, & \text{otherwise.} \end{cases}$$

Notice that  $\bar{\mu}_i^\omega \geq \tilde{\mu}_i^\omega (1 - \sigma_i \xi_i^\omega)$  for all  $i \in N$ . Moreover, the optimal solution value  $Q(\sigma, \omega) \geq \sum_{i \in N} \bar{u}_i^\omega$  as  $\tilde{\mathcal{S}}^\omega$  is a feasible solution. Let  $P = \{p_\omega\}_{\omega \in \Omega}$ . Then,

$$\begin{aligned} \Phi(\sigma) &= \max_{P \in \mathcal{P}} \sum_{\omega \in \Omega} p_\omega Q(\sigma, \omega) \\ &\geq \sum_{\omega \in \Omega} \tilde{p}_\omega \sum_{i \in N} \bar{u}_i^\omega \quad \because \{\tilde{p}_\omega\}_{\omega \in \Omega} \in \mathcal{P} \\ &\geq \sum_{\omega \in \Omega} \tilde{p}_\omega \sum_{i \in N} \tilde{\mu}_i^\omega (1 - \xi_i^\omega \sigma_i) \\ &= \Phi(\tilde{\sigma}) - \sum_{i \in N} \sum_{\omega \in \Omega} \tilde{p}_\omega \tilde{\mu}_i^\omega \xi_i^\omega \sigma_i, \end{aligned}$$

for any  $\sigma \in \mathcal{X}$ . This completes the proof.  $\square$

Next, we present a decomposition method that iteratively derives inequalities (2) to get tighter lower bound approximations of problem (1) in each iteration; refer to Algorithm 1 for its pseudocode. We initialize this algorithm by setting iteration counter  $L = 1$ , upper bound  $\theta^{ub} \leftarrow \infty$ , lower bound  $\theta^{lb} \leftarrow -\infty$ , and an initial feasible solution  $\tilde{\sigma}^1 \in \mathcal{X}$ . In iteration  $L \geq 1$ , we set  $\tilde{\sigma} = \tilde{\sigma}^L$  and solve the defender's problem for each scenario  $\omega \in \Omega$

in Line 4 to get  $Q(\tilde{\sigma}, \omega) = \sum_{i \in N} \tilde{\mu}_i^\omega$ . Then, in line 6 and 7, we get an extremal probability distribution  $\{\tilde{p}_\omega\}_{\omega \in \Omega}$ , an optimal solution of so-called distribution separation problem  $\max\{\sum_{\omega \in \Omega} p_\omega Q(\tilde{\sigma}, \omega) : \{p_\omega\}_{\omega \in \Omega} \in \mathcal{P}\}$ , and thereby, obtain  $\Phi(\tilde{\sigma}) = \sum_{\omega \in \Omega} \tilde{p}_\omega Q(\tilde{\sigma}, \omega)$ . If  $\Phi(\tilde{\sigma})$  is smaller than the best known upper bound  $\theta^{ub}$ , we update  $\theta^{ub}$  to  $\Phi(\tilde{\sigma})$  and the best known adversary's solution  $\tilde{\sigma}^*$  to  $\tilde{\sigma}$ . In Line 11, we add an inequality of the form (2) in  $\mathcal{M}^{L-1}$ , a lower-bound approximation of (1), to get  $\mathcal{M}^L$ :

$$\begin{aligned} \theta^{lb} &:= \min_{\sigma \in \mathcal{X}} \eta & (3) \\ \text{s.t. } \eta &\geq \Phi(\tilde{\sigma}) - \sum_{i \in N} \sum_{\omega \in \Omega} \tilde{p}_\omega \tilde{\mu}_i^\omega \xi_i^\omega \sigma_i, \text{ for } \tilde{\sigma} \in \{\tilde{\sigma}^1, \dots, \tilde{\sigma}^L\} \end{aligned}$$

which is a tighter lower bound approximation. Note that  $\mathcal{M}^0$  has no constraints other than constraints of  $\mathcal{X}$ . We solve  $\mathcal{M}^L$ ,  $L \geq 1$ , in Line 12 to get an optimal solution  $(\eta^{L+1}, \tilde{\sigma}^{L+1})$  and update the best-known lower bound  $\theta^{lb}$  to  $\eta^{L+1}$ . We terminate the algorithm when the optimality gap  $(\theta^{ub} - \theta^{lb})$  lies within a predetermined threshold  $\epsilon$ .

---

**Algorithm 1** Decomposition method for Problem (1)

---

- 1: Let  $L \leftarrow 1$ ,  $\theta^{lb} \leftarrow -\infty$ ,  $\theta^{ub} \leftarrow \infty$ ,  $\tilde{\sigma} \leftarrow \tilde{\sigma}^1 \in \mathcal{X}$ ;
- 2: **while**  $\theta^{ub} - \theta^{lb} > \epsilon$  **do**
- 3:     **for**  $\omega \in \Omega$  **do**
- 4:         Solve defender's problem to get  $Q(\tilde{\sigma}, \omega)$ ;
- 5:     **end for**
- 6:     Compute  $\{\tilde{p}\}_{\omega \in \Omega} = \arg \max_{P \in \mathcal{P}} \sum_{\omega \in \Omega} p_\omega Q(\tilde{\sigma}, \omega)$ ;
- 7:     Obtain  $\Phi(\tilde{\sigma}) = \sum_{\omega \in \Omega} \tilde{p}_\omega Q(\tilde{\sigma}, \omega)$ ;
- 8:     **if**  $\theta^{ub} > \Phi(\tilde{\sigma})$  **then**
- 9:          $\theta^{ub} \leftarrow \Phi(\tilde{\sigma})$  and  $\tilde{\sigma}^* \leftarrow \tilde{\sigma}$ ;
- 10:    **end if**
- 11:    Add the following inequality in  $\mathcal{M}^{L-1}$  to get  $\mathcal{M}^L$ :

$$\eta \geq \Phi(\tilde{\sigma}) - \sum_{i \in N} \sum_{\omega \in \Omega} \tilde{p}_\omega \tilde{\mu}_i^\omega \xi_i^\omega \sigma_i;$$

- 12:    Solve  $\mathcal{M}^L$  to get optimal solution  $(\eta^{L+1}, \tilde{\sigma}^{L+1})$ ;
  - 13:    Update the lower bound  $\theta^{lb} \leftarrow \eta^{L+1}$  and  $\tilde{\sigma} \leftarrow \tilde{\sigma}^{L+1}$ ;
  - 14:     $L \leftarrow L + 1$ ;
  - 15: **end while**
  - 16: **Return:**  $\theta^{ub}, \tilde{\sigma}^*$
- 

**Observation 2.1.** *Inequality (2) is tight (which implies satisfied at equality) for  $\sigma = \tilde{\sigma}$ , i.e.,  $\sum_{\omega \in \Omega} \tilde{p}_\omega \sum_{i \in N} \tilde{\mu}_i^\omega \xi_i^\omega \tilde{\sigma}_i = 0$ . This is because for each  $i \in N$ , either  $\xi_i^\omega \tilde{\sigma}_i = 0$  (request not impacted by attack) or  $\tilde{\mu}_i^\omega = 0$  (covered reward is zero, in case request is successfully attacked).*

**Theorem 2.2.** *Algorithm 1 solves problem (1) in a finite number of iterations if there exist finitely convergent algorithms to compute  $Q(\hat{\sigma}, \omega)$  for each  $(\hat{\sigma}, \omega) \in \mathcal{X} \times \Omega$ , and to solve problem  $\max\{\sum_{\omega \in \Omega} p_\omega Q(\hat{\sigma}, \omega) : \{p_\omega\}_{\omega \in \Omega} \in \mathcal{P}\}$ .*

*Proof.* In iteration  $L$  of Algorithm 1, we add an optimality cut to  $\mathcal{M}^{L-1}$  and solve it (a mixed binary program) using branch-and-cut algorithm that is finitely convergent. If solving  $\mathcal{M}^L$  provides an adversary's solution  $\tilde{\sigma}^L$  that was also found in iteration  $K < L$ , then  $\tilde{\sigma}^L$  is an optimal solution because Observation (2.1) leads to  $\theta^{lb} = \theta^{ub}$ . Otherwise, since  $|\mathcal{X}|$  is finite, the algorithm converges in finite iterations.  $\square$

**Remark 2.1.** *Conditions of Theorem 2.2 are automatically satisfied when: (a)  $\mathcal{P}$  is a polytope (e.g. moment matching set), and (b) CFP is solved in finite iterations.*

### 3 Algorithms for Single Camera View-Frame Placement Problem

We study the single camera view-frame placement problem (denoted by S-CFP). The objective of S-CFP is to find the position and resolution level of the camera view-frame  $s = [(x_s, y_s), w_s, h_s, z_s]$  to maximize the reward covered by  $s$ , i.e.,

$$\max_{x_s, y_s, z_s} \left\{ f(x_s, y_s, z_s) = \sum_{i \in N} g(\alpha_i) r_i A(d_i \cap s) \right\}.$$

**Definition 3.1** (Base Vertex [15]). *Given request  $d_i = [(x_i, y_i), w_i, h_i, r_i, z_i]$ , we define  $x_{left}^i = x_i$ ,  $x_{right}^i = x_i + w_i$ ,  $y_{bot}^i = y_i$  and  $y_{top}^i = y_i + h_i$  for  $i \in N$ . Then, the set of all base vertices  $\mathcal{B}$  from requests  $\{d_i\}_{i \in N}$  is given by:*

$$\mathcal{B} := \{(x, y) : x \in \{x_{left}^i, x_{right}^i\}_{i \in N}, y \in \{y_{bot}^j, y_{top}^j\}_{j \in N}\}.$$

*In simple words, a base vertex (BV) corresponds to a corner of a request or intersection of extended edges of any two requests.*

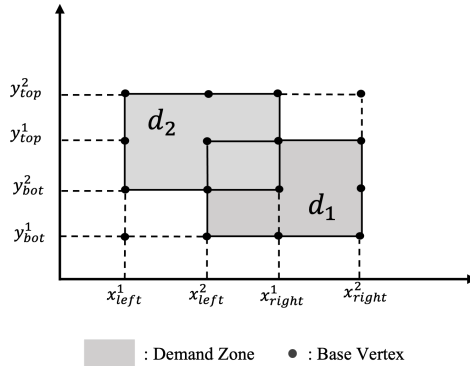


Figure 1: Illustration of BVs when two requests  $d_1$  and  $d_2$  are given.

**Lemma 3.1** ([15]). *For a given instance of S-CFP and any fixed resolution  $\hat{z}_s \in \mathbb{R}_+$ , there exists an optimal solution  $\hat{s} = [(\hat{x}_s, \hat{y}_s), \hat{w}_s, \hat{h}_s, \hat{z}_s]$  such that either of the following conditions are satisfied:*

- (a)  $(\hat{x}_s, \hat{y}_s) \in \mathcal{B}$ ,
- (b)  $(\hat{x}_s + \hat{w}_s, \hat{y}_s) \in \mathcal{B}$ ,
- (c)  $(\hat{x}_s, \hat{y}_s + \hat{h}_s) \in \mathcal{B}$ ,
- (d)  $(\hat{x}_s + \hat{w}_s, \hat{y}_s + \hat{h}_s) \in \mathcal{B}$ .

*Exact Algorithms for S-CFP.* Lemma 3.1 reduces the solution space for the location of the camera view-frame from continuous space ( $\mathbb{R}^2$ ) to a discrete set of BVs, such that an optimal solution has one of its corner at a BV. Song et al. [15] introduced two exact algorithms for S-CFP, referred as BV algorithm and BV-IC algorithm that work as follows. In each iteration, a corner of the frame is placed at a BV as per Lemma 3.1 and then derive a univariate piecewise polynomial function of  $z_s$ . (The breakpoints of this polynomial function of  $z_s$  are called critical  $z$  values.) Using an explicit description of each piece of this function, it is maximized to get a feasible solution for the original problem. This process is repeated until all the cases of Lemma 3.1 are explored.

The subsequent proposition further reduces the solution search space for S-CFP by proving that it is sufficient to place a corner at BVs in a subset of  $\mathcal{B}$  to get an optimal solution. We refer to BV and BV-IC algorithms where a corner of the frame is placed at a BV based on this theorem as Improved BV and Improved BV-IC algorithms. From our computational experiments, we observe that this theoretical result reduces the run time of the algorithms in [15] for S-CFP by up to 68%.

**Proposition 3.1.** *For a given instance of S-CFP and any fixed resolution  $\hat{z}_s \in \mathbb{R}_+$ , there exists an optimal frame  $\hat{s} = [(\hat{x}_s, \hat{y}_s), \hat{w}_s, \hat{h}_s, \hat{z}_s]$  such that either of the following conditions are satisfied:*

- (a)  $(\hat{x}_s, \hat{y}_s) \in \mathcal{B}_1$ ,
- (b)  $(\hat{x}_s + \hat{w}_s, \hat{y}_s) \in \mathcal{B}_2$ ,
- (c)  $(\hat{x}_s, \hat{y}_s + \hat{h}_s) \in \mathcal{B}_3$ ,
- (d)  $(\hat{x}_s + \hat{w}_s, \hat{y}_s + \hat{h}_s) \in \mathcal{B}_4$ ,

where  $\mathcal{B}_1 \cup \mathcal{B}_2 \cup \mathcal{B}_3 \cup \mathcal{B}_4 = \mathcal{B}$ , and

$$\begin{aligned} \mathcal{B}_1 &:= \{(x, y) : x \in \{x_{left}^i\}_{i \in N}, y \in \{y_{bot}^j\}_{j \in N}\} \subset \mathcal{B}, \\ \mathcal{B}_2 &:= \{(x, y) : x \in \{x_{right}^i\}_{i \in N}, y \in \{y_{bot}^j\}_{j \in N}\} \subset \mathcal{B}, \\ \mathcal{B}_3 &:= \{(x, y) : x \in \{x_{left}^i\}_{i \in N}, y \in \{y_{top}^j\}_{j \in N}\} \subset \mathcal{B}, \\ \mathcal{B}_4 &:= \{(x, y) : x \in \{x_{right}^i\}_{i \in N}, y \in \{y_{top}^j\}_{j \in N}\} \subset \mathcal{B}. \end{aligned}$$

**Remark 3.1.** *This result is similar to Theorem 2 of [2] that is written in the context of a facility location problem. However, in [2], the resolution is fixed and therefore, the implications of reduced search space on (S-)CFP with varying resolution levels have not been evaluated.*

## 4 Approximation Algorithm and Heuristics for Multi Cameras View-Frame Problem

In this section, we present three solution approaches for CFP with multiple cameras, i.e.,  $p \geq 2$  (denoted by M-CFP).

**Greedy Algorithm.** Similar to the generic greedy-framework, we solve S-CFP multiple ( $p$ ) times sequentially to get a feasible solution for M-CFP. We prove that the approximation ratio of this approach is  $1 - 1/e$  where  $e$  is the base of natural logarithm, i.e., it provides a solution whose objective value is at least  $1 - 1/e$  times the optimal solution value. Interestingly, this result is applicable for CFP with any two-dimensional spatial object (circle, polygon, etc.) as request and view-frame. Therefore, we first introduce the following notations to incorporate this generality.

**Definition 4.1.** Let  $\mathcal{D}_j^g$  be a set of (general) requests that is an input to S-CFP in the  $j^{\text{th}}$  iteration of the greedy algorithm. Also, let  $\psi_j^g$  denotes the optimal covered reward returned by (general) view-frame  $s_j$  for  $\mathcal{D}_j^g$ .

**Observation 4.1.** Since  $\psi_j^g$  is the optimal objective value of S-CFP with  $\mathcal{D}_j^g$  as input,  $p\psi_j^g$  provides an upper bound for the optimal solution value of the  $p$  camera view-frame placement problem when its input is  $\mathcal{D}_j^g$ , denoted by  $\zeta_j^g$ , i.e.,  $p\psi_j^g \geq \zeta_j^g$ .

**Theorem 4.1.** Let  $\gamma_g$  denotes the approximation ratio for the greedy algorithm, i.e., ratio of the objective value of the greedy solution and optimal objective value of general M-CFP. Then

$$\gamma_g > 1 - \frac{1}{e} \quad (4)$$

where  $e$  is the base of natural logarithm.

*Proof.* Let the optimal solution value for (general) M-CFP be denoted by  $f^*$ . Then, the approximation ratio is given by

$$\gamma_g = \frac{1}{f^*} \left( \sum_{l=1}^p \psi_g^l \right). \quad (5)$$

Note that for  $j = 1$ ,  $\mathcal{D}_1^g = \mathcal{D}$  and hence  $\zeta_1^g = f^*$ . Also, since after each iteration  $l \in \{1, \dots, j-1\}$  of the greedy algorithm, we trim out the requests of total reward  $\psi_g^l$ , we get,

$$p\psi_g^j \geq \zeta_j^g \geq f^* - \sum_{l=1}^{j-1} \psi_g^l \quad (6)$$

where  $\psi_g^0 = 0$ . This implies,

$$\begin{aligned} p \sum_{l=1}^j \psi_g^l &\geq f^* + (p-1) \sum_{l=1}^{j-1} \psi_g^l \\ &\geq f^* \left( 1 + \frac{p-1}{p} + \left( \frac{p-1}{p} \right)^2 + \dots + \left( \frac{p-1}{p} \right)^{j-1} \right). \end{aligned}$$

By setting  $j = p$  in the foregoing inequality, we derive

$$\gamma_g = \frac{1}{f^*} \left( \sum_{l=1}^p \psi_g^l \right) \geq \left( 1 - \left( \frac{p-1}{p} \right)^p \right) \quad (7)$$

Because the function in the right-hand side of the inequality is decreasing in  $p$ , we can get the limit of this function as  $p$  approaches infinity, i.e.,  $\gamma_g > 1 - 1/e$ .  $\square$

Iterative Extreme BV Algorithm. To obtain a solution better than the greedy solution, we present a heuristic for M-CFP with two rectangular view-frames and  $n$  rectangular requests where a corner of each frame lies at an extreme BV.

**Definition 4.2.** *Let*

$$\begin{aligned} x_{max} &= \max\{x_{right}^i : i \in N\}, \quad x_{min} = \min\{x_{left}^i : i \in N\}, \\ y_{max} &= \max\{y_{top}^i : i \in N\}, \quad y_{min} = \min\{y_{bot}^i : i \in N\}. \end{aligned}$$

*We define a set of extreme BVs as follows:*

$$\mathcal{EB} = \{(x, y) \in \mathcal{B} : x \in \{x_{max}, x_{min}\} \text{ or } y \in \{y_{min}, y_{max}\}\}.$$

We place view-frame at one of extreme BVs based on Theorem 3.1, derive corresponding set of critical  $z$  values, and pick a critical  $z$  value as resolution level of the view-frame.

For the second camera, we solve S-CFP using improved BV algorithm with only extreme BVs to determine the position and resolution level of the second view-frame. We store the summation of the reward captured by both frames. However, in case there is a subregion covered by both frames, only the reward captured by the frame that provides better resolution/reward is included in the solution value. We repeat this process for each extreme BV and associated critical  $z$  values as a solution for the first view-frame.

Clustering Algorithm. To deal with M-CFP instances with large number of requests and camera view-frames, we divide the set of requests into multiple ( $\leq p$ ) clusters (or subsets of requests), and solve S-CFP or M-CFP with  $p_1 < p$  cameras for each cluster in parallel.

## 5 Heuristic Method for Multi-Cameras View-Frame Placement Problem with Fixed Tilt of Cameras

In this section, we present a heuristic algorithm for CFP with cameras having continuous resolution levels, while the tilt of cameras (i.e.,  $y$  coordinate of their view-frames) are fixed and their  $x$  coordinates belong to a predetermined set of candidate locations  $\mathcal{L} = \{x_{l_1}, \dots, x_{l_m}\}$ . Since the cameras have fixed and same tilt, the M-CFP is equivalent to 1-dimensional problem where requests and view-frames are represented by line segments. This problem (denoted by M-CFP-F) arise in surveillance of borders, streets, and rivers, among other narrow regions. In the ensuing sections, we examine the challenges involved in addressing M-CFP-F and propose a branch and bound-based heuristic that outperforms other heuristics in terms of solution quality. Assume that  $w_{s_0}$  is base width such that  $w_{s_j} = w_{s_0} z_{s_j}$  for  $j \in \{1, \dots, p\}$ .

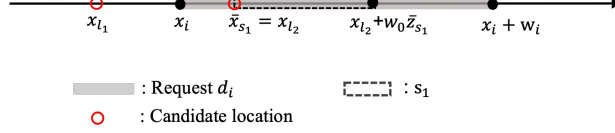


Figure 2: An example of request  $d_i$  overlapping with view-frame  $s_1$

## 5.1 Theoretical Properties for M-CFP-F

In fig. 2, we consider a request  $d_i$ , view-frame  $s_1$  with fixed x-coordinate  $\bar{x}_{s_1}$  and resolution level  $\bar{z}_{s_1}$ , and view-frame  $s_2$  with only fixed x-coordinate  $\bar{x}_{s_2} = x_{l_1}$ . We analyze covered-reward function  $f_i(x_s, z_s)$  with respect to  $z_{s_2}$ . We observe that function  $f_i(\bar{x}_{s_1}, \bar{x}_{s_2}, \bar{z}_{s_1}, z_{s_2})$  has six breakpoints, referred to as  $z$ -critical values:

$$\left( \frac{x_i - \bar{x}_{s_2}}{w_{s_0}}, \frac{x_i + w_i - \bar{x}_{s_2}}{w_{s_0}}, z_i, \frac{\bar{x}_{s_1} - \bar{x}_{s_2}}{w_{s_0}}, \frac{\bar{x}_{s_1} + w_{s_0} \bar{z}_{s_1} - \bar{x}_{s_2}}{w_{s_0}}, \bar{z}_{s_1} \right) \quad (8)$$

In (8), there are two types of critical  $z$  values. The first type of critical  $z$  values are generated by the presence of request  $d_i$ , and are denoted as zRCVs. The second type of critical  $z$  values are generated by the existence of a fixed view-frame,  $s_1$ , and are referred to as zFCVs. A formal definition of both subsets of the  $z$  critical values is provided below.

**Definition 5.1.** (*zRCVs*) For any  $x_{l_k} \in \mathcal{L}$ , the set of  $z$ -critical values generated by the request  $d_i$  is defined by

$$\mathcal{Z}_{d_i, x_{l_k}} = \left\{ \frac{x_i - x_{l_k}}{w_{s_0}}, \frac{x_i + w_i - x_{l_k}}{w_{s_0}}, z_i \right\}.$$

We denote set of all zRCVs for all elements in  $\mathcal{L}$  by

$$\mathcal{Z}_R = \cup_{i \in N} \cup_{x_{l_k} \in \mathcal{L}} \mathcal{Z}_{d_i, x_{l_k}}.$$

**Definition 5.2.** (*zFCVs*) Let  $\{s_j\}_{j \in \mathcal{J}}$  be the set of camera view-frames with known position  $x_{s_j}$  and resolution  $z_{s_j}$  where  $\mathcal{J} \subset P = \{1, \dots, p\}$ . We define zFCVs generated by  $s_j, j \in \mathcal{J}$  and  $x_{l_k} \in \mathcal{L}$  as follows.

$$\mathcal{Z}_{s_j, x_{l_k}} = \left\{ \frac{x_{s_j} - x_{l_k}}{w_{s_0}}, \frac{x_{s_j} + w_{s_0} z_{s_j} - x_{l_k}}{w_{s_0}}, z_{s_j} \right\}. \quad (9)$$

Thus, for  $\{s_j\}_{j \in \mathcal{J}}$ , we define the set of all zFCVs as

$$\mathcal{Z}(\mathcal{J}) = \cup_{j \in \mathcal{J}} \cup_{x_{l_k} \in \mathcal{L}} \mathcal{Z}_{s_j, x_{l_k}}.$$

For 2-CFP-F, notice that function  $f_i(\bar{x}_{s_1}, \bar{x}_{s_2}, \bar{z}_{s_1}, z_{s_2}) = \mathcal{R}(d_i \cap s_1) + \mathcal{R}(d_i \cap s_2) - \mathcal{R}_{12}^i$  where  $\mathcal{R}(d_i \cap s_2) = r_i A(d_i \cap s_2) \times \min\left(\frac{z_i}{z_{s_2}}, 1\right)$ ,

$$\mathcal{R}_{12}^i = \mathcal{R}(d_i \cap s_1 \cap s_2) = r_i A(d_i \cap s_1 \cap s_2) \times \min\left(\frac{z_i}{\bar{z}_{s_1}}, \frac{z_i}{z_{s_2}}, 1\right)$$

and  $\mathcal{R}(d_i \cap s_1)$  is constant. Since

$$\begin{aligned} A(d_i \cap s_2) &= \{\min(x_i + w_i, \bar{x}_{s_2} + w_{s_0} z_{s_2}) - \max(x_i, \bar{x}_{s_2})\}^+ \\ A(d_i \cap s_1 \cap s_2) &= \{\min(x_i + w_i, \bar{x}_{s_1} + w_{s_0} \bar{z}_{s_1}, \bar{x}_{s_2} + w_{s_0} z_{s_2}) \\ &\quad - \max(x_i, \bar{x}_{s_1}, \bar{x}_{s_2})\}^+, \end{aligned}$$

where operator  $a^+$  returns  $a$  if  $a > 0$  and 0 if  $a \leq 0$ , function  $f_i(\bar{x}_{s_1}, \bar{x}_{s_2}, \bar{z}_{s_1}, z_{s_2})$  can be written as

$$f_i(\bar{x}_{s_1}, \bar{x}_{s_2}, \bar{z}_{s_1}, z_{s_2}) = g_0 z_{s_2} + g_1 z_{s_2}^{-1} + g_2$$

where coefficients  $g_0, g_1$  and  $g_2$  known.

If  $g_1 \geq 0$ , then  $f_i'' \geq 0$  which implies that the function is convex. Also, if  $g_1 < 0$  and  $g_0 \geq 0$ , then  $f_i' \geq 0$  and  $f_i'' < 0$ . This implies that the function is a non-decreasing concave function. For both cases, when a interval  $[z_{t_1}, z_{t_2}]$  is given, defined by the two consecutive  $z$ -critical values, the function  $f_i(\bar{x}_{s_1}, \bar{x}_{s_2}, \bar{z}_{s_1}, z_{s_2})$  attains maximum value within the interval at  $z_{t_1}$  and/or  $z_{t_2}$ . Therefore, it suffices to consider the set of  $z$ -critical values to obtain the optimal solution.

**Observation 5.1.** *Coefficients  $g_0 < 0$  and  $g_1 < 0$  only when*

$$\begin{aligned} A(d_i \cap s_2) &= w_{s_0} z_{s_2} - (\bar{x}_{s_1} - \bar{x}_{s_2}), \\ A(d_i \cap s_1 \cap s_2) &= w_{s_0} z_{s_2} - (\bar{x}_{s_2} - \max(x_i, \bar{x}_{s_1}, \bar{x}_{s_2})) \end{aligned}$$

and  $\bar{z}_{s_1} \geq z_{s_2} \geq z_i$ . Also, if  $g_0 < 0$  and  $g_1 < 0$  then  $g_0 = -r_i w_{s_0} z_i / \bar{z}_{s_1}$  and  $g_1 = -r_i (x_i - \bar{x}_{s_2}) z_i$ .

In this case, the function is non-increasing concave function if following two assumptions holds.

*Assumption 1:* There is an upper bound  $q$  for the resolution level of the view frame, which implies that width of each view-frame cannot exceed  $w_{s_0} q$ .

*Assumption 2:* Request  $d_i$  is assumed to be covered only by a view-frame positioned at the candidate point  $x_{i_k} \in \mathcal{L}$  that satisfies  $x_i - x_{i_k} \leq \frac{w_{s_0} z_i^2}{q}$ . This implies that no reward is covered if the quality of coverage is below a certain threshold.

However, when considering request  $d_j$  whose resolution  $z_j$  satisfies  $z_i \leq z_{s_2} \leq z_j \leq \bar{z}_{s_1}$ ,

$$\begin{aligned} f(\bar{x}_{s_1}, \bar{x}_{s_2}, \bar{z}_{s_1}, z_{s_2}) &= \left( r_j w_{s_0} - \frac{r_j w_{s_0} z_j}{\bar{z}_{s_1}} - \frac{r_i w_{s_0} z_i}{\bar{z}_{s_1}} \right) z_{s_2} \\ &\quad - \frac{r_i (x_i - \bar{x}_{s_2})}{z_{s_2}} + g_2' \end{aligned}$$

for some constant  $g_2'$ . Even with the assumptions we made, the presence of the stationary point within the interval  $[z_i, z_j]$  of the objective function depends on problem parameters, such as reward rate and desired resolution. As a result, considering only  $z$ -critical values for the view-frame  $s_2$  may lead to non-optimal solution, which in turn makes it challenging to define a discrete solution space (that contains an optimal solution) for addressing M-CFP-F.

## 5.2 Heuristic Algorithm for M-CFP-F

This section presents a heuristic method based on branch-and-bound framework for solving M-CFP-F. We assume that the solution space for resolution of camera view frames is restricted to zRCVs and zFCVs, and there exists a camera view-frame  $s_1$  (wlog) such that  $z_{s_1}$  is a zRCV. To implement, we partition the entire set of feasible solutions (root node) of M-CFP-F into smaller subsets (child nodes) and evaluate the smaller solution spaces by computing their upper bounds. If a current node (reduced solution space) cannot provide a solution better than the best solution obtained so far, we eliminate this node (pruning). The overall methodology and terminology are similar to the algorithms discussed in [2], however, we have modified the data structure and functions for our problem. The major difference arises from the nature of the  $z$ -critical values. While in the algorithm presented in [2] the values of  $x$ - and  $y$ -FCVs that need to be considered for unfixed frames are the same in the algorithm, in our problem, for each candidate location  $x_{l_k} \in \mathcal{L}$ , different values of zFCVs must be considered.

To begin, a greedy algorithm is applied to get an initial feasible solution and the lower bound. The root node, denoted as  $V_0$ , is then established, containing  $p$  sets of elements from  $\mathcal{L}$  and  $\mathcal{Z}_R$ , with the  $j^{\text{th}}$  set representing the solution space for the  $j$ -th view-frame ( $j \in \{1, \dots, p\}$ ). Further information regarding the procedure and data structure can be found in [2]. In the following, we briefly provide overall data structure and key functions of this algorithm for M-CFP-F.

### 5.2.1 Upper Bound Function

For each  $x_{l_j} \in \mathcal{L} = \{x_{l_1}, \dots, x_{l_m}\}$ , we calculate the set of zRCVs,  $Z^j = \{z_{q_1}^j, \dots, z_{q_j}^j\}$  where  $q_j$  is the number of zRCV defined by  $x_{l_j}$ . Then, we obtain the possible covered reward when we locate the single view-frame at  $x_{l_j}$  with the resolution  $z \in Z^j$ . We complete this process for all  $x_{l_j} \in \mathcal{L}$  and construct a matrix  $M$  whose rows and columns are indexed by the set of  $x_{l_j} \in \mathcal{L}$ ,  $j \in \{1, \dots, l_m\}$  and  $z_q \in \mathcal{Z}_R$ ,  $q \in \{1, \dots, |\mathcal{Z}_R|\}$ , where  $M(x_{l_j}, z_q)$  returns reward covered by a view-frame when located at  $(x_{l_j}, z_q)$ . Note that  $M(x_{l_j}, z_q) = 0$  if  $z_q \notin Z^j$ . The remaining steps to obtain upper bound follows from [2].

### 5.2.2 Branching

The process of generating child nodes of the current node is called branching. We first branch along with the  $x$  axis to determine the locations of the  $p$  view frames. After the  $x$  coordinate of each frame has been fixed to one of the elements in  $\mathcal{L}$ , branching continues along the  $z$  axis to determine the resolution of each frame. As per assumption we made, the solution space of the resolution for each frame is established. Whenever we fix the resolution of one of the frames, we calculate the zFCVs that are needed to be considered for each  $x_{l_k} \in \mathcal{L}$  and these zFCVs are taken into account when determining the resolution of frames whose resolution has not yet been determined.

## 6 Computational Results for Random Instances

In this section, we present the results of our computational experiments on randomly generated instances to evaluate the performance of algorithms for adversarial CFP (Section 6.1) and CFP with single and multiple cameras (Section 6.2). We generate these instances as follows [2, 15]: In  $1000 \times 1000$  region, we randomly generate three seed points with a circular range of radius 270. There are 93% chances that the lower-left corner of a request is generated within a circular range of these three seed points and 7% chances that it will be anywhere in the entire region. Additionally,  $w_i, l_i \sim \text{uniform}(5,50)$ ,  $z_i \sim \text{uniform}(1,10)$ , and  $r_i \sim \text{uniform}(1,30)$  for all  $i \in N$ . We also randomly generate a realization  $\xi^\omega \in \{0,1\}^n$ ,  $\omega \in \Omega$  from the Bernoulli distribution with probability 0.75, i.e.,  $\xi_i^\omega = 1$  with probability 0.75. For the moment-matching ambiguity set, we set  $m = 1$ ,  $l_1 = 0.95 \sum_{\omega \in \Omega} \xi^\omega / |\Omega|$  and  $u_1 = 1.05 \sum_{\omega \in \Omega} \xi^\omega / |\Omega|$ , i.e., bounds on first-moment. We implement all algorithms in Python using Gurobi 9.1 as optimization solver on a machine with Intel Xeon(R) W-2255 processor (3.7 GHz) and 32GB RAM.

### 6.1 Computational Results for Adversarial CFP

We conduct computational experiments on instances with different number of requests  $n \in \{10, 15, 20\}$ , number of target frames  $p \in \{2, 3, 4, 5\}$ , and the attackers’ budget  $b \in \{2, 3, 4, 5\}$ . For each combination of  $(n, p, b)$ , we generate 10 instances and report average over results for these instances in Table 1. For  $|\Omega| = 100$ , the column labeled as “DRA-CFP” reports the distributionally risk-averse solution value, which is the expected covered reward by the defender for the worst-case probability distribution, and solution time (in seconds). To emphasize the significance of the distributionally robust solution, we introduce the Value of the Distributionally robust Solution (VDS) that is computed as follows. For a given instance, let  $\sigma^*$  and  $\Phi(\sigma^*)$  be an optimal solution of Problem (1) and the optimal solution value, respectively. Assuming that all attacks are successful, i.e.,  $\xi_i^\omega = 1$  for all  $i \in N$  and  $\omega \in \Omega$ , we solve the foregoing instance and get a deterministic optimal solution, denoted by  $\hat{\sigma}_D \in \mathcal{X}$ , with  $\phi_D$  as associated solution value. We report  $\phi_D$  and  $\Phi(\hat{\sigma}_D)$  after averaging over 10 instances with same  $(n, p, b)$  in Table 1. Note that  $\Phi(\hat{\sigma}_D)$  returns the expected reward covered after adversary’s action  $\hat{\sigma}_D$  but in the presence of uncertainty. Now,

$$\text{VDS} = \Phi(\hat{\sigma}_D) - \Phi(\sigma^*),$$

where VDS equal to zero implies that the deterministic solution when considered in uncertain environment leads to same covered reward as given by the optimal solution value of Problem (1). In Table 1, we report average VDS only for instances with  $\text{VDS} > 0$ . The positive VDS can be analyzed from two different perspectives.

**Interdictor’s Perspective.** Assume that we pick the deterministic model, Problem (1) with  $\xi_i^\omega = 1$  for all  $(\omega, i)$ , to decide interdiction actions  $\hat{\sigma}_D$  against an enemy and its agents with the goal of minimizing the maximum information the enemy can cover. In such case, even though the optimal covered reward  $\phi_D$  reported by the deterministic model is always better than  $\Phi(\sigma^*)$ , the “realistic” covered reward after incorporating uncertainty in the success of attacks  $\Phi(\hat{\sigma}_D) > \Phi(\sigma^*)$  when VDS is positive. In other

$n$	$p$	$b$	Deterministic	DRA-CFP			VDS	# of instances VDS>0
			Reward $\phi_D$	Reward $\Phi(\sigma^*)$	Time(s)	$\Phi(\hat{\sigma}_D)$		
10	2	2	388	523	12	529.5	6.5	3
		3	317	465	12.3	477.3	12.3	2
		4	299	416	11.7	429.3	13.3	3
		5	260	372	11.7	409.7	37.7	4
	3	2	768	907	24.0	925.6	18.6	3
		3	629	820	23.3	865.1	45.1	3
		4	560	793	23.2	807.9	14.9	4
		5	395	781	20.1	848.3	67.3	4
	4	2	1083	1227	36.0	1241.8	14.1	4
		3	941	1160	36.3	1168.3	8.3	4
		4	703	1131	39	1220.9	89.9	3
		5	546	1112	33.3	1287.8	175.8	4
	5	2	1526	1678	51.6	1751.0	73	3
		3	1159	1451	54.0	1462.5	11.5	3
		4	847	1434	48.1	1448.2	14.2	3
		5	721	1362	45.2	1520.4	158.4	4
	2	2	621	722	47.7	777.5	55.5	3
		3	462	644	46.9	671.6	27.6	3
		4	400	608	43.7	643.4	35.4	4
		5	358	577	44.1	612.7	35.7	4
3	2	953	1015	80.7	1103.5	88.5	3	
	3	818	926	85.9	1043.9	117.9	4	
	4	668	913	83.6	1051.0	138	3	
	5	613	877	77.9	921.2	44.2	3	
4	2	1384	1522	131.4	1572.6	50.6	3	
	3	1265	1460	132.8	1486.8	26.8	5	
	4	1095	1412	133.6	1484.6	72.6	4	
	5	1025	1392	122.2	1497.5	105.5	6	
5	2	1622	2048	194.6	2137.8	89.8	6	
	3	1557	1948	220.9	2045.9	97.9	7	
	4	1192	1944	231.6	2072.8	128.8	6	
	5	1061	1868	223.1	2205.0	337	8	
2	2	788	802	122.8	868.7	66.7	6	
	3	683	787	129.6	828.4	41.4	4	
	4	679	740	118.3	807.7	67.7	6	
	5	563	717	110.4	814.5	97.5	5	
3	2	1189	1203	194.2	1321.3	118.3	5	
	3	1063	1089	196.8	1213.1	124.1	7	
	4	1019	1045	199.7	1126.5	81.5	6	
	5	851	1008	196.1	1093.0	85	5	
4	2	1667	1731	297.6	1791.0	60	5	
	3	1482	1720	340.4	1830.0	110	6	
	4	1447	1696	350.3	1810.0	114	8	
	5	1226	1591	303.3	1663.0	72	6	
5	2	2025	2143	396.1	2197.0	54	4	
	3	1875	2122	482.4	2207.0	85	6	
	4	1826	1999	496.4	2097.0	98	5	
	5	1566	1875	410.8	2055.5	180.5	8	

Table 1: Computational Results for the Adversarial CFP (1)

words, the enemy covers more reward when as an interdictor we do not incorporate uncertainty.

**Defender’s Perspective.** In contrast, selecting the deterministic model as a defender to analyze an adversary’s actions mislead the defender in two ways: (a) The defender is overly cautious and overestimating the risk-appetite of the adversary, and (b) For an adversary using model (1), the deterministic solution might not be optimal and therefore, they would opt  $\sigma^*$  actions as  $\Phi(\sigma^*) < \Phi(\hat{\sigma}_D)$  when VDS is positive. From our computational experiments, we observe that for 92 out of 160 instances with  $n = 20$ ,  $\sigma^*$  is different from  $\hat{\sigma}_D$ . This impacts defenders vulnerability analysis as well.

## 6.2 Computational Results for CFP without Adversary

We computationally evaluate the impact of the reduced search space (Theorem 3.1) on the performance of two exact algorithms for S-CFP in [15], referred as BV algorithm and BV-IC algorithm. We also evaluate effectiveness of proposed solution approaches for M-CFPs.

### 6.2.1 Results for S-CFP

In Table 2, each row also reports an average over 10 randomly generated instances. Columns labelled as “BV” and “BV-IC” report solution time (in seconds) of the BV and BV-IC algorithms, respectively, of [15]. Whereas, columns labelled as “Impr BV” and “Impr BV-IC” report solution time (in seconds) of these approaches with the reduced search space, according to Theorem 3.1. We report the reduction in computational time for each algorithm as improvement, i.e.,  $100 \times (1 - T_I/T_O)$  where  $T_O$  and  $T_I$  indicate the time taken by the original algorithm and improved algorithm, respectively. We observe that the improvement increases as the number of requests are increased, with more than 50% reduction in run time for  $n \geq 30$ . Moreover, Figure 3 shows that when  $n \leq 100$ , the improved BV algorithm outperforms original BV-IC algorithm even though it is an upgraded version of BV algorithm proposed in the [15].

$n$	BV $T_O(s)$	Impr BV $T_I(s)$	Improvement %	BV-IC $T_O(s)$	Impr BV-IC $T_I(s)$	Improvement %
10	0.1	0.06	40	0.08	0.04	50
30	7.5	2.9	60	4.5	2.0	54
50	58	21	64	29	12	59
70	235	81	65	104	42	60
90	713	242	66	284	111	61
100	1,165	386	67	441	171	61
150	7,171	2,313	68	2,198	827	62
200	27,102	8,473	68	7,074	2,595	63
250	77,716	24,387	68	17,998	6,736	62

Table 2: Computational results for S-CFP

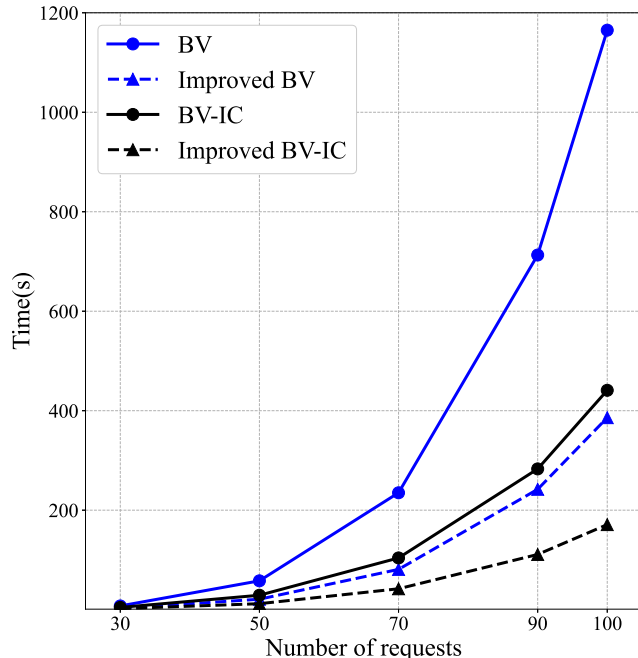


Figure 3: Impact of Theorem 3.1 on performance of algorithms for S-CFP

### 6.2.2 Results for M-CFP using Approximation Algorithm and Heuristics

In Table 3, we compare the performance of greedy approach and extreme BV approach for  $p = 2$  and  $n \in \{5, 10, \dots, 30\}$ . As expected, the former is computationally efficient but the latter provides better solution and reward coverage. We can observe that the increase in  $n$  and  $p$  significantly increase the time taken by the greedy method. Recall that in the clustering approach, the set of requests is divided into multiple clusters. We utilize  $k$ -means clustering approach to create  $p$  clusters and then solve S-CFP for each cluster using Improved BV-IC algorithm (both in series and in parallel). Based on table 3, this approach (even without parallel computing) is much faster in comparison to the greedy method. For example, for  $n = 500$ , the greedy algorithm takes more than 6100 seconds to position 10 frames, in comparison to 66 seconds taken by the clustering approach. Moreover, the latter covers 99.9% of the reward covered by the former. In the worst case, when  $n = 400$ , the clustering approach covers 87% of the reward covered by greedy method, but it takes only 0.67% of the time taken by greedy method.

### 6.2.3 Computational Results for M-CFP-F

We present the computational result for the M-CFP-F instances with continuous resolution and  $\mathcal{L}$  as the set of candidate locations. Each row reports an average of 10 instances. We compare the three algorithms, branch and bound based heuristic, greedy algorithm and clustering based algorithm by reporting solution time and relative reward percentage (denoted by RelRew) assuming the reward captured by the heuristic is 100. The reward

$n$	$p$	Greedy		Clustering			Extreme BV	
		Reward	Time (s)	Reward	Time (s) in parallel	Time (s) in series	Reward	Time (s)
5		1,061	0.01	885	3.00	0.03	1,072	1.37
10		1,160	0.12	939	2.00	0.04	1,247	113
20	2	1,497	1.12	1,239	2.47	0.13	1,501	3,350
30		1,553	4.42	1352	2.13	0.41	1,826	3600+
50		1,661	22.31	1590	2.03	2.41	1,960	3600+
100		7,216	244	8,026	3.2	0.8		
200		13,430	1,089	12,983	4.6	8.0		
300	10	17,139	2,787	15,991	12	31	N/A	
400		22,891	4301	19,984	29	88		
500		25,365	6101	25,055	66	204		

Table 3: Computational results for M-CFP: Greedy, Clustering and Extreme BV Methods

$p$	$n$	$ \mathcal{L} $	Heuristic Algorithm		Greedy approach			Clustering Approach		
			Time	Reward	Time	Reward	RelRew(%)	Time	Reward	RelRew(%)
3	10	7	24	1002	0.002	863	86	0.02	797	79
		10	33	1295	0.003	1166	90	0.02	1121	86
		7	1216	1548	0.02	1323	86	0.03	1165	75
	20	10	1339	1750	0.03	1629	93	0.03	1301	74
		15	1156	2090	0.03	1753	84	0.03	1324	63
		10	11816	3277	0.25	2931	89	0.03	2300	70
50	15	13,701	4074	0.28	3702	90	0.03	3090	75	
	20	14,745	4172	0.32	3799	91	0.03	3141	75	

Table 4: Computational Results for M-CFP-F

reported by the greedy approach is at least 84% (on average) of the reward reported by the heuristic, in comparison to 132% by the clustering approach. In terms of solution time, the cluster approach performs better than the greedy and heuristic algorithms. Note that the clustering approach is a heuristic so it does not provide any guarantee the quality of solution.

## 7 Case Study

In this section, we present a case study to emphasize the effectiveness of the improved algorithms for CFP and to also highlight the practicality of the camera view-frame placement problem. The overall procedure of this case study is based on the framework (Hydra) proposed by [4] to find a hidden object in a remote area using CFP. Below we provide a brief summary of this framework that consists of the following steps.

1. **Requests Generation:** Given a set of  $n$  automated agents, each agent generates a rectangular request based on its own probability distribution to detect the hidden object. Specifically, an agent generates request that maximizes the information gain calculated based on its current probability distribution. Note that the probability distribution of the agent is initialized by the Dirichlet process and updated in the last step of each iteration.
2. **Placing Optimal Camera View Frame** Given the set of  $n$  requests, optimal pan, tilt, and zoom for multiple cameras (installed on aerial vehicles) is obtained by solving CFP, M-CFP, or M-CFP-F.
3. **Termination Conditions.** The automated agents check whether or not the hidden object lies within the subregions captured by the camera view-frames. Since there is a possibility of false negative, the iteration will terminate when the hidden object is captured by a camera with predetermined desired resolution level for the object.
4. **Update Probability Distributions** If automated agents conclude that a hidden object is not detected, they update their own probability distribution by Bayes' rule. This updated probability distribution is used for generating requests in the next iteration.

*Computational Results.* In Table 5, we report average number of iterations and time taken to find a hidden object using BV-IC and improved BV-IC algorithms for S-CFP. We consider  $25 \times 25$  and  $50 \times 50$  search areas. Since both are exact algorithms, the number of iterations is same for both of them. However, as expected, we reduce computational time by using improved BV-IC algorithm for placing the optimal camera view-frames.

## 8 Conclusion

We introduced adversarial CFP in the presence of uncertainty in the success of attacks and distributional ambiguity. The proposed algebraic modeling framework allowed adjustments based on risk-appetite of the decision makers. We presented valid inequalities to derive lower

$p$	Search Areas	$n$	BV-IC		Improved BV-IC	
			#Iterations	Time (s)	#Iterations	Time (s)
1	$25 \times 25$	5	6.0	0.05	6.0	0.03
		7	3.8	0.03	3.8	0.02
	$50 \times 50$	15	17.8	20.2	17.8	11.0
		20	19.6	24.2	19.6	12.1

Table 5: Computational result for simulation study: Hydra

bound approximations for the objective function and a decomposition algorithm to solve it to optimality. We proved finite convergence of this decomposition algorithm.

We conducted extensive computational experiments to emphasize the utility of this problem and the solution approach. Moreover, we studied CFP with single or multiple cameras (denoted by S-CFP and M-CFP, respectively), but in the absence of adversary and uncertainty. We strengthened the theoretical properties introduced in [15] for S-CFP, and as a result, we further reduced the solution search space and improved the computational efficiency of algorithms for the S-CFP. We used these algorithms within a simulation framework – Hydra – to find a hidden object. For M-CFP, we proposed: (a) an approximation algorithm for  $p = 2$ , (b) a Greedy algorithm with approximation ratio of  $1 - 1/e$ , (c) a clustering based heuristics, and (d) another heuristic algorithm when tilt of cameras is fixed and their pan belongs to a finite set of values. Again, we computationally evaluated performance of these approaches along with the quality of solution.

## References

- [1] Manish Bansal, Kuo-Ling Huang, and Sanjay Mehrotra. “Decomposition algorithms for two-stage distributionally robust mixed binary programs”. In: *SIAM Journal on Optimization* 28.3 (2018), pp. 2360–2383.
- [2] Manish Bansal and Kiavash Kianfar. “Planar maximum coverage location problem with partial coverage and rectangular demand and service zones”. In: *INFORMS Journal on Computing* 29.1 (2017), pp. 152–169.
- [3] Manish Bansal and Yingqiu Zhang. “Scenario-based cuts for structured two-stage stochastic and distributionally robust p-order conic mixed integer programs”. In: *Journal of Global Optimization* 81.2 (2021), pp. 391–433.
- [4] Ephrat Bitton and Ken Goldberg. “Hydra: A framework and algorithms for mixed-initiative UAV-assisted search and rescue”. In: *2008 IEEE International Conference on Automation Science and Engineering*. IEEE, 2008, pp. 61–66.
- [5] Richard L Church. “The planar maximal covering location problem.(Symposium on location problems: in memory of Leon Cooper)”. In: *Journal of regional science Philadelphia* 24.2 (1984), pp. 185–201.
- [6] Delbert Ray Fulkerson and Gary C Harding. “Maximizing the minimum source-sink path subject to a budget constraint”. In: *Mathematical Programming* 13.1 (1977), pp. 116–118.

- [7] Gerd Hirzinger, Bernhard Brunner, Johannes Dietrich, and Johann Heindl. “Sensor-based space robotics-ROTEX and its telerobotic features”. In: *IEEE Transactions on robotics and automation* 9.5 (1993), pp. 649–663.
- [8] Eitan Israeli and R Kevin Wood. “Shortest-path network interdiction”. In: *Networks: An International Journal* 40.2 (2002), pp. 97–111.
- [9] Sumin Kang and Manish Bansal. “Distributionally risk-receptive and risk-averse network interdiction problems with general ambiguity set”. In: *Networks* 81.1 (2023), pp. 3–22.
- [10] Jaques Marescaux and Francesco Rubino. “Transcontinental robot-assisted remote telesurgery, feasibility and potential applications”. In: *Teleophthalmology* (2006), pp. 261–265.
- [11] Abraham Mehrez and Alan Stulman. “The maximal covering location problem with facility placement on the entire plane”. In: *Journal of Regional Science* 22.3 (1982), pp. 361–365.
- [12] Alan T Murray and Daoqin Tong. “Coverage optimization in continuous space facility siting”. In: *International Journal of Geographical Information Science* 21.7 (2007), pp. 757–776.
- [13] Douglas A Samuelson. “Changing the war with Analytics: top US intelligence officer in Central Asia recommends massive overhaul of how information is gathered and utilized”. In: *OR/MS Today* 37.3 (2010), pp. 30–36.
- [14] Dezhen Song and Kenneth Y Goldberg. “Approximate algorithms for a collaboratively controlled robotic camera”. In: *IEEE Transactions on Robotics* 23.5 (2007), pp. 1061–1070.
- [15] Dezhen Song, A Frank van der Stappen, and Ken Goldberg. “Exact algorithms for single frame selection on multiaxis satellites”. In: *IEEE Transactions on Automation Science and Engineering* 3.1 (2006), pp. 16–28.
- [16] CDT Watson-Gandy. “Heuristic procedures for the m-partial cover problem on a plane”. In: *European Journal of Operational Research* 11.2 (1982), pp. 149–157.
- [17] Richard Wollmer. “Removing arcs from a network”. In: *Operations Research* 12.6 (1964), pp. 934–940.
- [18] Yiliang Xu and Dezhen Song. “Systems and algorithms for autonomously simultaneous observation of multiple objects using robotic ptz cameras assisted by a wide-angle camera”. In: *2009 IEEE/RSJ International Conference on Intelligent Robots and Systems*. IEEE. 2009, pp. 3802–3807.
- [19] Yiliang Xu, Dezhen Song, and Jingang Yi. “Exact algorithms for non-overlapping 2-frame problem with non-partial coverage for networked robotic cameras”. In: *2010 IEEE International Conference on Automation Science and Engineering*. IEEE. 2010, pp. 503–508.

- [20] Yiliang Xu, Dezhen Song, Jingang Yi, and A Frank Van Der Stappen. “An approximation algorithm for the least overlapping p-frame problem with non-partial coverage for networked robotic cameras”. In: *2008 IEEE International Conference on Robotics and Automation*. IEEE. 2008, pp. 1011–1016.